Supplementary Material

Development of dipeptide *N*-acetyl-L-cysteine loaded nanostructured carriers based on inorganic layered hydroxides

Denise Eulálio,[1] Mariana Pires Figueiredo,[1] Christine Taviot-Gueho,[2,3] Fabrice Leroux,[2,3] Cristina Helena dos Reis Serra,[4] Dalva Lúcia Araújo de Faria[1] and Vera Regina Leopoldo Constantino[1*]

[1] Departamento de Química Fundamental, Instituto de Química, Universidade de São Paulo - USP, Av. Prof. Lineu Prestes 748, CEP 05508-000, São Paulo, SP, Brazil.
[2] Université Clermont Auvergne, Institut de Chimie de Clermont-Ferrand, BP 10448, F-63000 Clermont-Ferrand, France.
[3] CNRS, UMR 6296, ICCF, F-63178 Aubiere, France.
[4] Departamento de Farmácia, Faculdade de Ciências Farmacêuticas, Universidade de São Paulo - USP, Av. Prof. Lineu Prestes 580, CEP 05508-000, São Paulo, SP, Brazil.

***** Correspondence: vrlconst@iq.usp.br (V.R.L.C.); Tel.:+55 (11) 3091-9152

Content

1. XRD patterns of LDH-NAC samples and NAC polymorphs

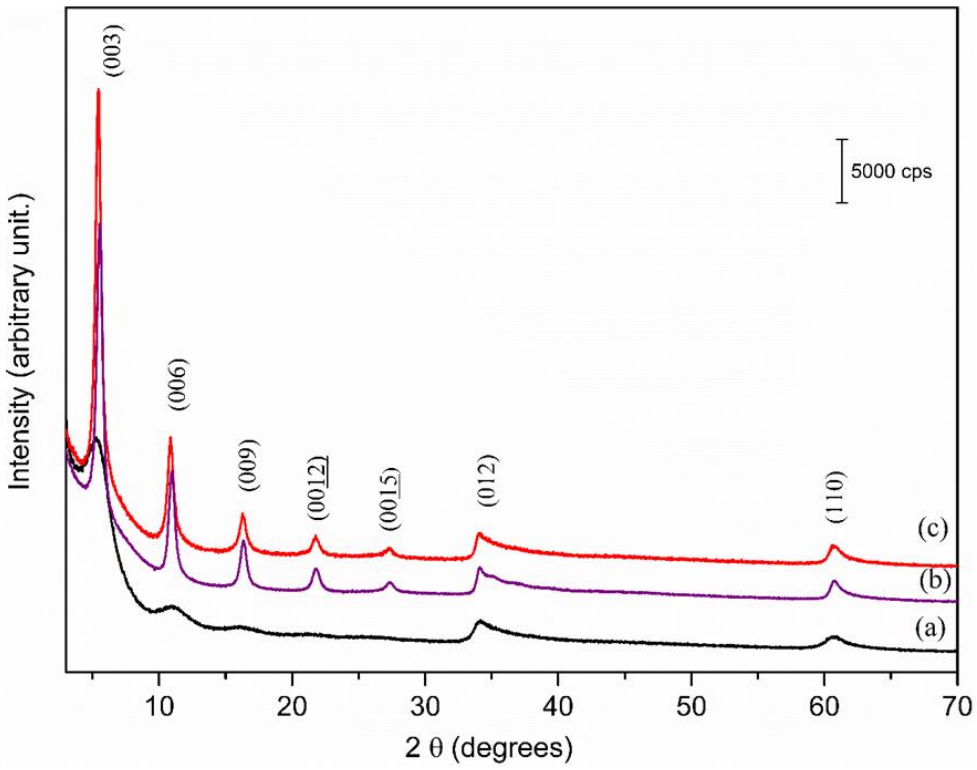

Figure S1. XRD patterns of LDH-NAC synthesized under distinct experimental conditions: (a) Zn_2Al-NAC (room temperature and NAC/Al molar ratio =1), (b) Zn_2Al-NAC55 (55 °C and NAC/Al molar ratio =1), and (c) Zn_2Al-1.3NAC55 (55 °C and NAC/Al molar ratio =1.3).

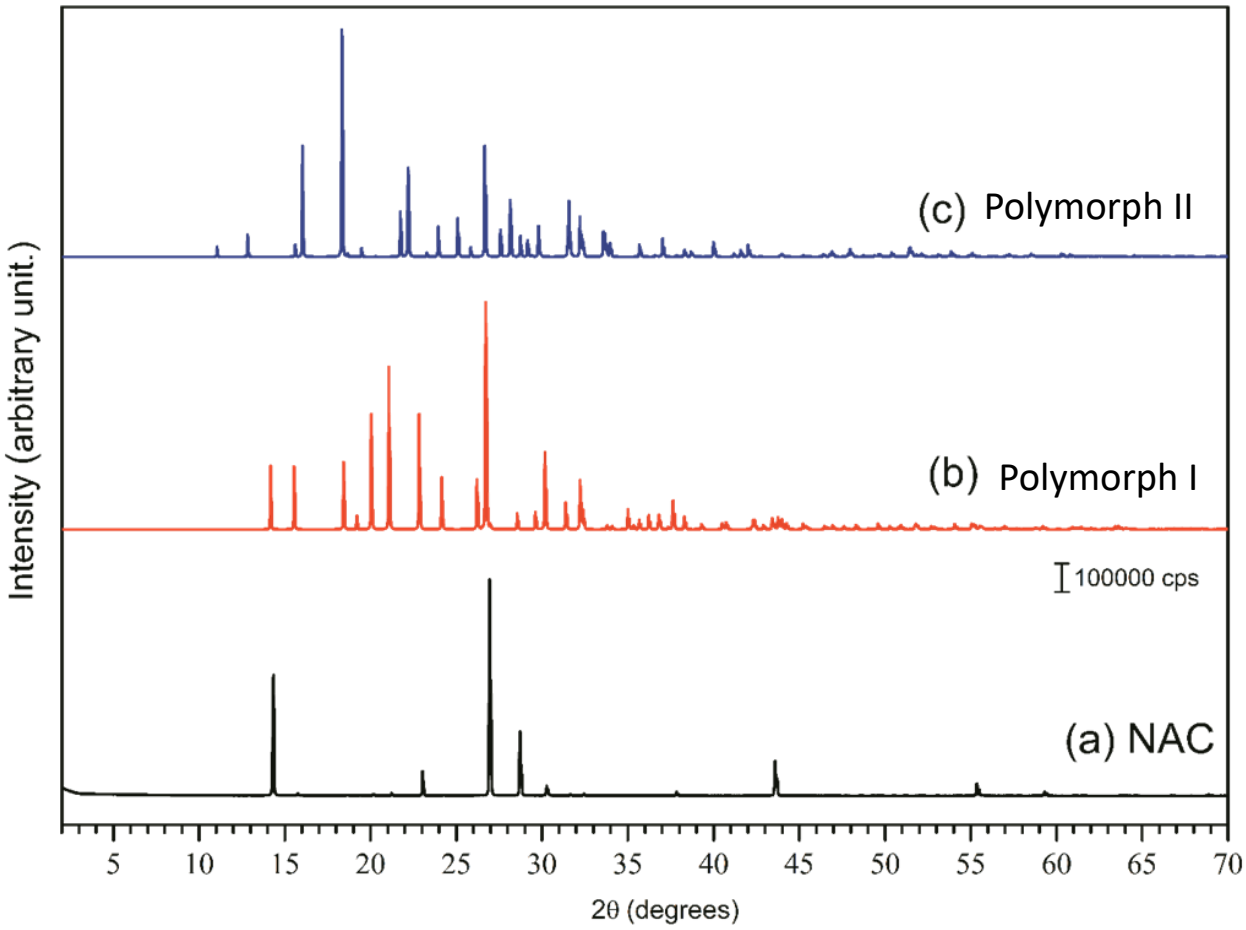

Figure S2. Comparison between XRD patterns of (a) NAC used in this work, (b) Polymorph I and (c) Polymorph II.

2. Crystal structure of NAC polymorphs obtained by XRD

Polymorph I structure comprises intermolecular interactions between NH•••S (2.82 Å), OCOH•••O=C (1.65 Å), and CH•••OCOH (2.72 Å), and intramolecular interaction between NH•••OCOH (2.26 Å).[1] Polymorph II shows intermolecular interactions of NH•••S (2.97 Å), OCOH•••O=C (1.66 Å), and CH•••OCOH (2.36 Å) and SH•••OCOH (2.15 Å). NAC used in this work is the polymorph I.

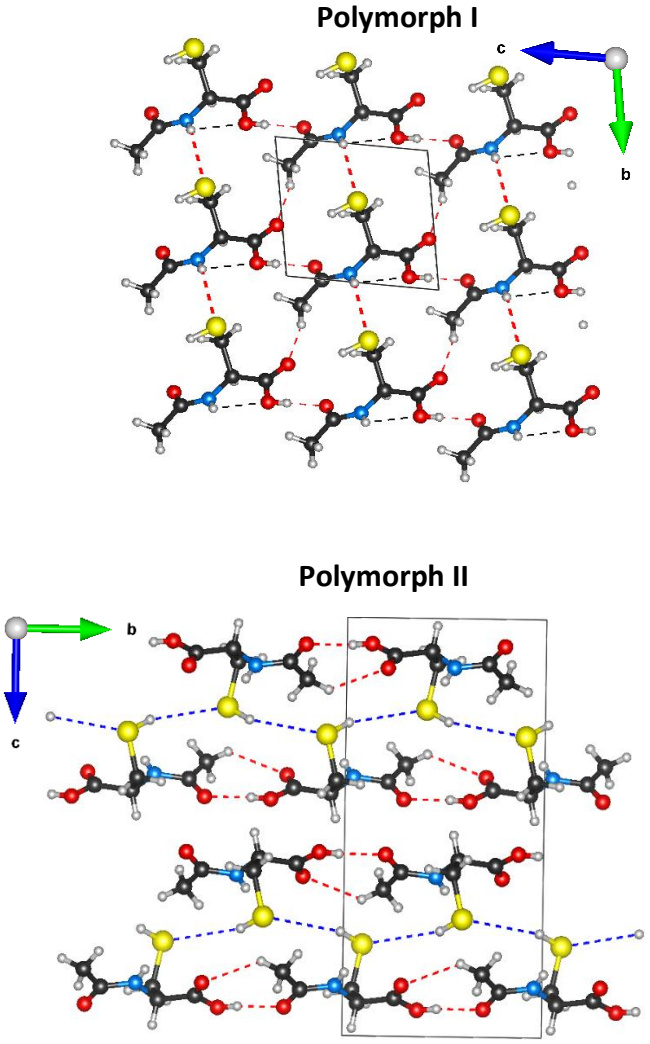

Figure S3. Crystalline packaging of polymorphs I and II, obtained in the Vesta version 3 program, from the crystallographic data deposited at Cambridge Crystallographic Data Centre by Kumar e Nagia [1].

3. Speciation curves for NAC species relative to pH value

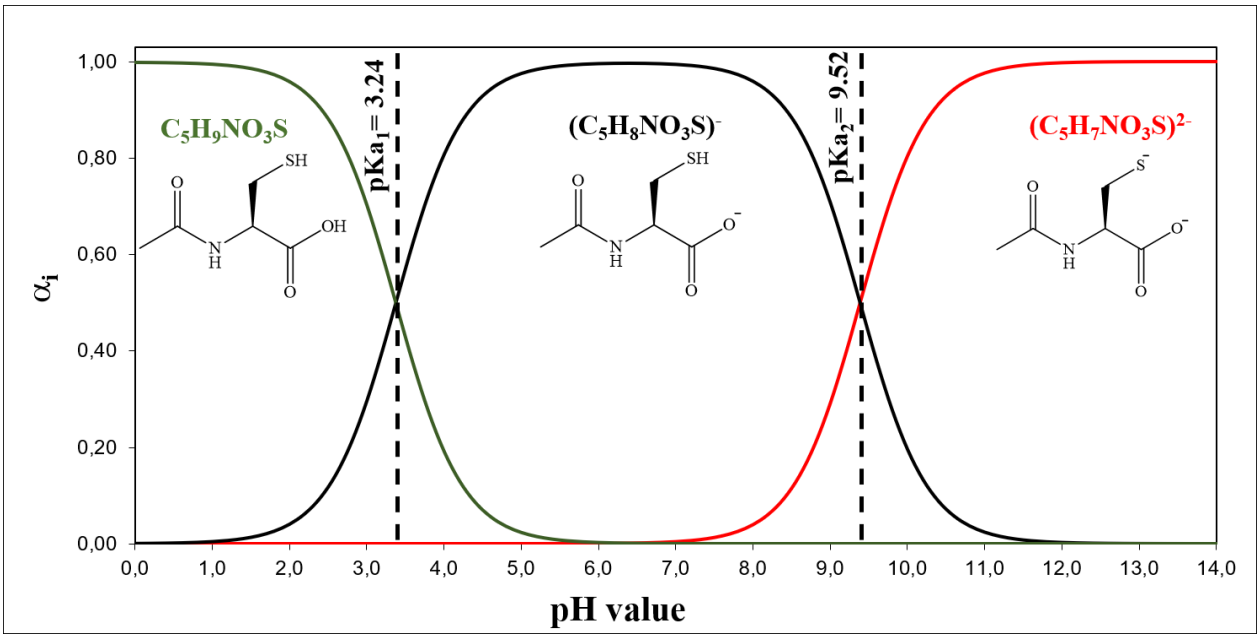

Figure S4. Curves of distribution of NAC species, where α_i is the species fraction, obtained through the *CurTiPOt* program, developed by Prof. Dr. Ivano G. R. Gutz, from Instituto de Química - USP.

4. FTIR and FT-Raman spectra of NAC samples obtained by freeze-drying of solutions in different pH values

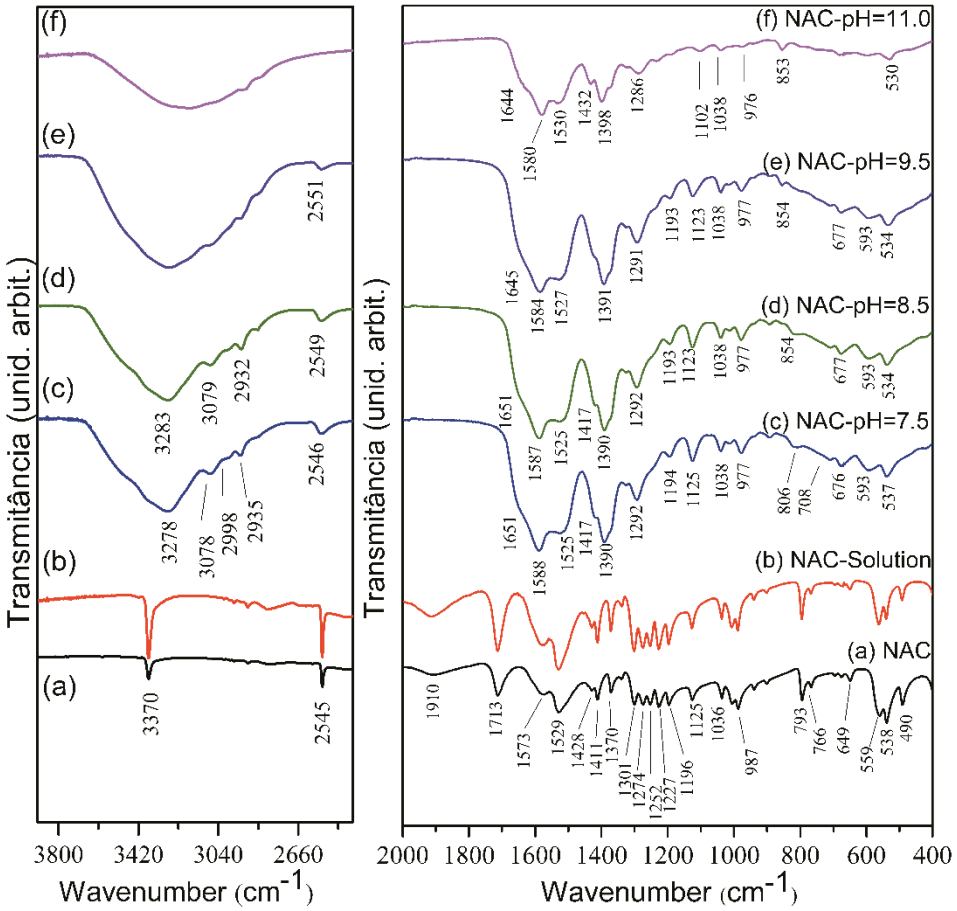

Figure S5. FTIR spectra of (a) NAC, (b) NAC dissolved in water and posteriorly freeze-dried, (c) NAC-pH=7.5, (d) NAC-pH=8.5, (e) NAC-pH=9.5, and (f) NAC-pH=11.

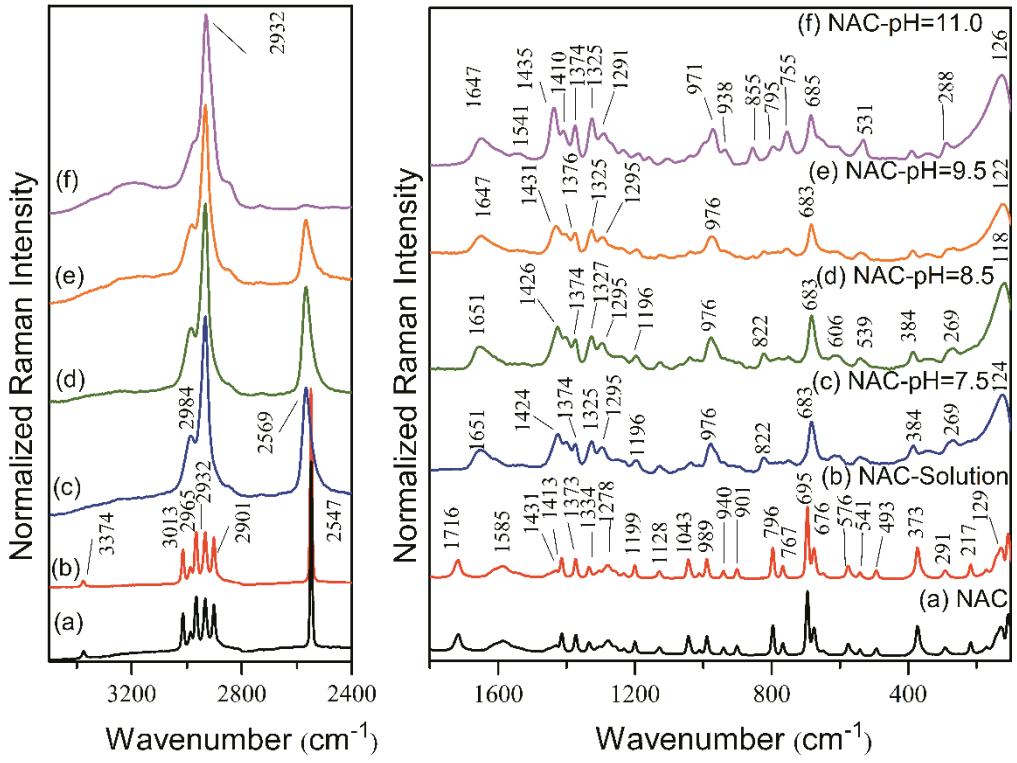

Figure S6. FT-Raman spectra of (a) NAC, (b) NAC dissolved in water and posteriorly freeze-dried, (c) NAC-pH=7.5, (d) NAC-pH=8.5, € NAC-pH=9.5, and (f) NAC-pH=11.

Table S1. IR and Raman band positions (in cm^{-1}) of NAC (polymorph I), NAC-pH=11.0, Zn_2Al-NAC55 and their tentative assignment.

NAC		NAC-pH=11		Zn_2Al-NAC55		Tentative assignment
FTIR	**Raman**	**FTIR**	**Raman**	**FTIR**	**Raman**	
3370	3374					ν N-H
				3322		ν O-H
	3013					ν_{as} C-H (CH_3)
	2965					ν_{as} C-H (CH_2)
	2932	2932	2932			ν_s C-H (CH_3)
	2901				2932	ν_s C-H (CH_2)
2545	2547					ν S-H
1713	1716					ν C=O (COOH)
				1628		δ H_2O
1573	1585(b)	1644	1647			ν C=O (amide)
		1580		1574		ν_{as} COO^-
1529		1525		1528		δ N-H
					1429	δ CH_2
		1398		1394	1399	ν_s COO^-
1274	1278	1286	1291	1292	1287	ν C-N
	695	680(w)	685		683	ν C-S
					124	δ O-Zn-O

a) ν = stretching, δ = bending, s = symmetric, as = antisymmetric

b) (b) = broad; (w) = weak

5. Thermal analysis data of NAC and NAC-pH=11 samples

NAC melts at 120°C (endothermic peak) and decomposes in two main events (**Figure S7**). XRD pattern of NAC used in this work is assigned to the polymorph I. The first event has a $T_{initial}$ value equal to 130 °C (DTG peaks at 198 and 216 °C) and the second equal to 440 °C (DTG peak at 559 °C); in both events occur the loss of H_2O, CO_2, and SO_2 molecules. No residue is noticed after the sample heated up to 1000 °C.

The thermal analysis data of NAC-pH=11 sample shows the loss of hydration water molecules from room temperature up to about 200 °C, followed by the decomposition step ($T_{initial}$= 220 °C, DTG peak at 252 °C) (**Figure S7**). The release of CO_2 above 700 °C indicates the formation of an intermediate carbon species.

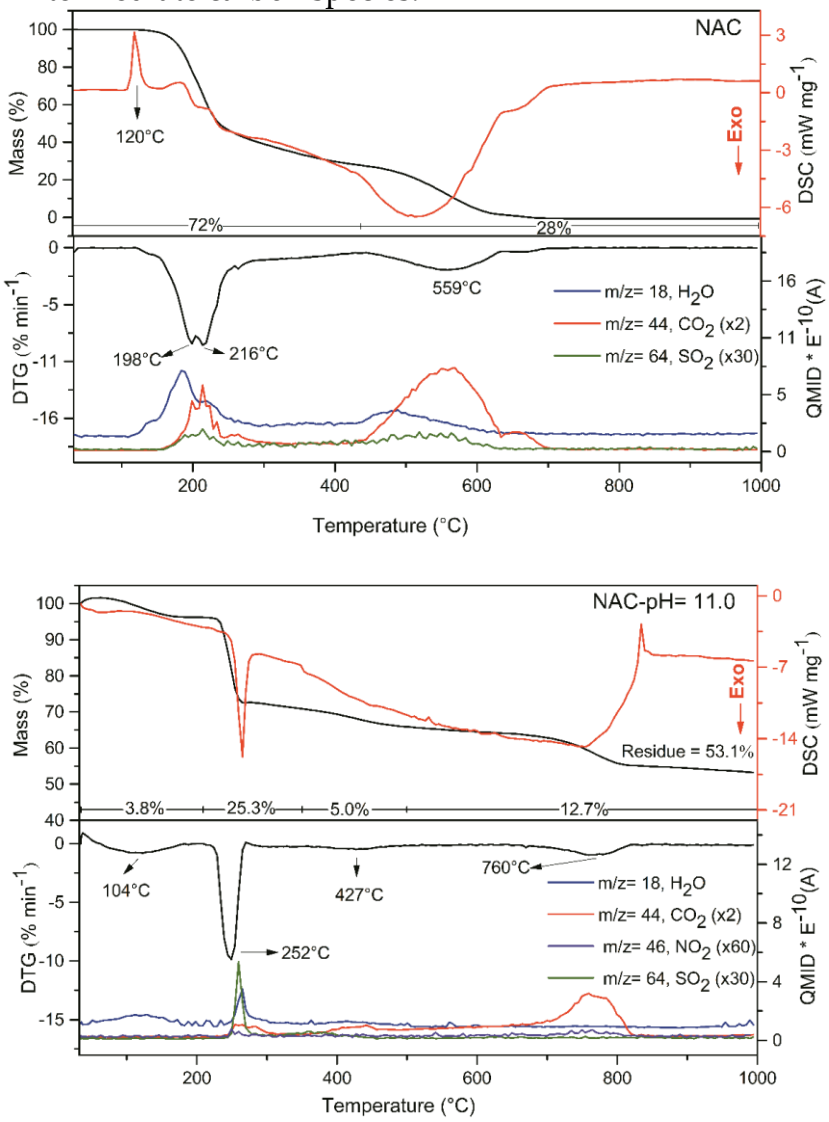

Figure S7. TG/DSC and DTG-MS curves of NAC polymorph I (top) and NAC-pH=11 samples (down).

6. Thermal analysis data of Zn_2Al-Cl55 sample

The assignment of the events occurring in the thermal decomposition of Zn_2Al-Cl (shown in **Figure S8**) was previously reported [2]. The amount of HCl released from dehydrochlorination is low and could not be identified in the experimental conditions applied in this work.

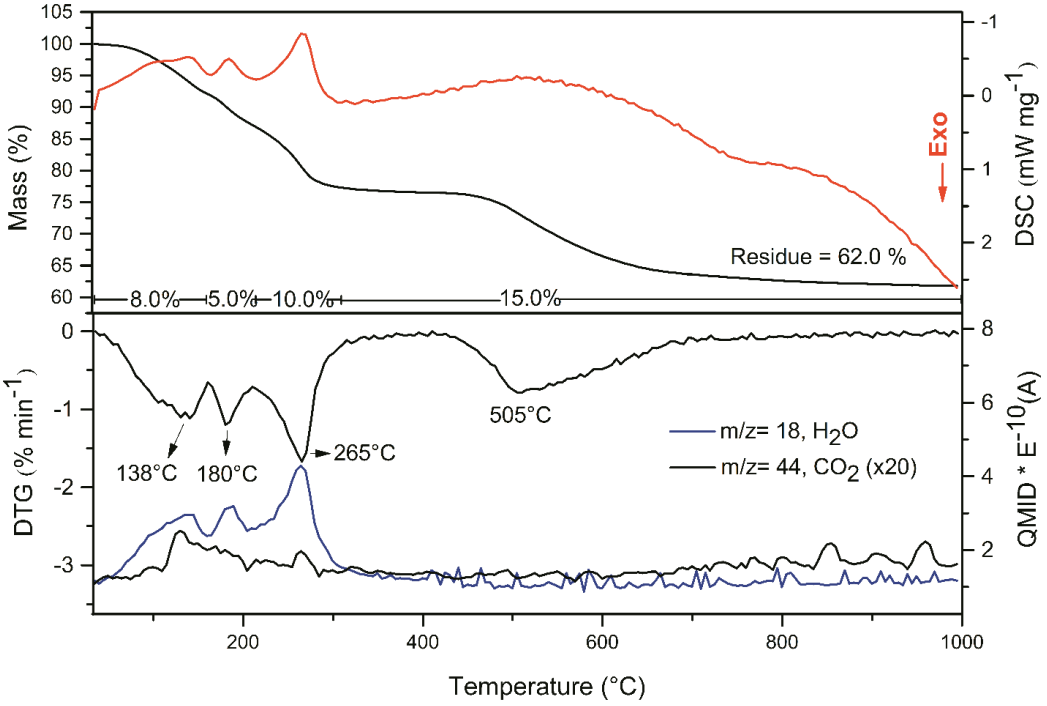

Figure S8. TG/DSC and DTG-MS curves of Zn_2Al-Cl55 sample under atmospheric air.

7. XRD patterns of Mg_2Al-NAC samples obtained at different synthetic parameters

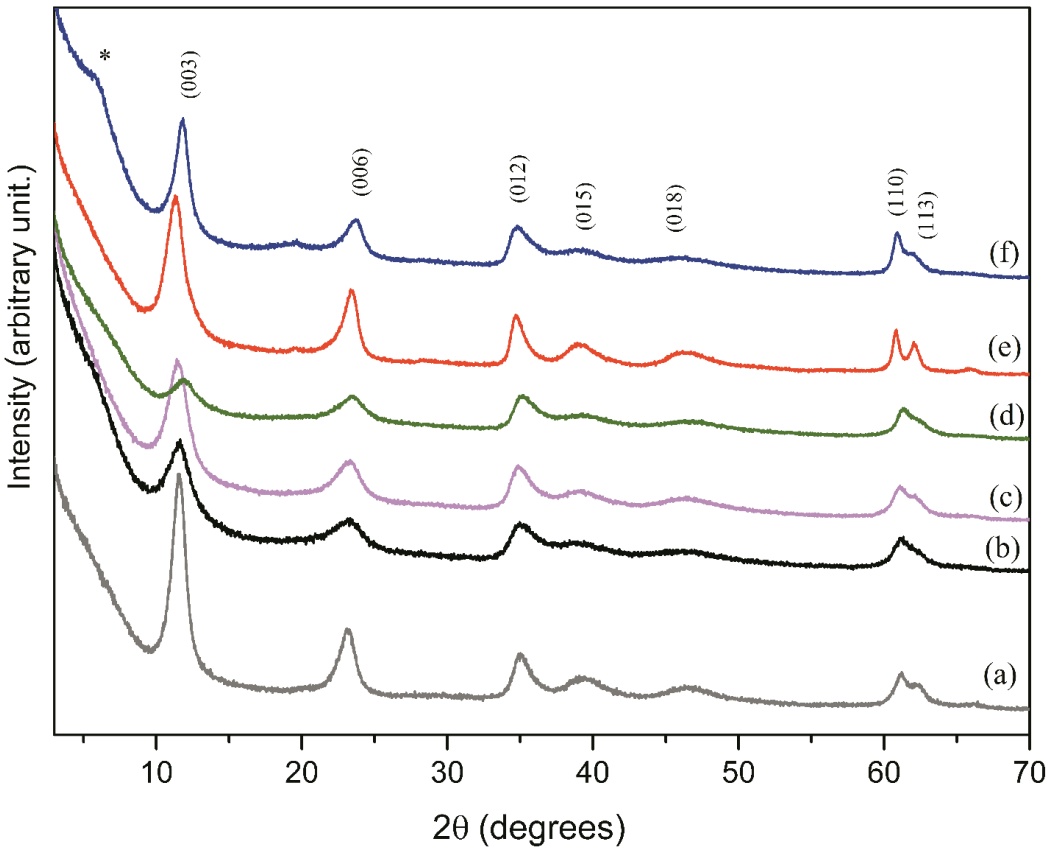

Figure S9. XRD patterns of (a) Mg_2Al-Cl (b) Mg_2Al-NAC (synthesis described in the Experimental section), (c) Mg_2Al-0.5NAC (NAC/Al^{3+} molar ratio used in the synthesis = 0.5), (d) Mg_2Al-2NAC (NAC/Al^{3+} molar ratio used in the synthesis = 2) (e) Mg_2Al-NAC_90_24h (aging process at 90°C for 24 h) and (f) Mg_2Al-NAC55 (synthesis described in Experimental section). (*) equipment artefact.

8. FTIR and Raman spectra of Mg_2Al-NAC and Mg_2Al-Cl samples

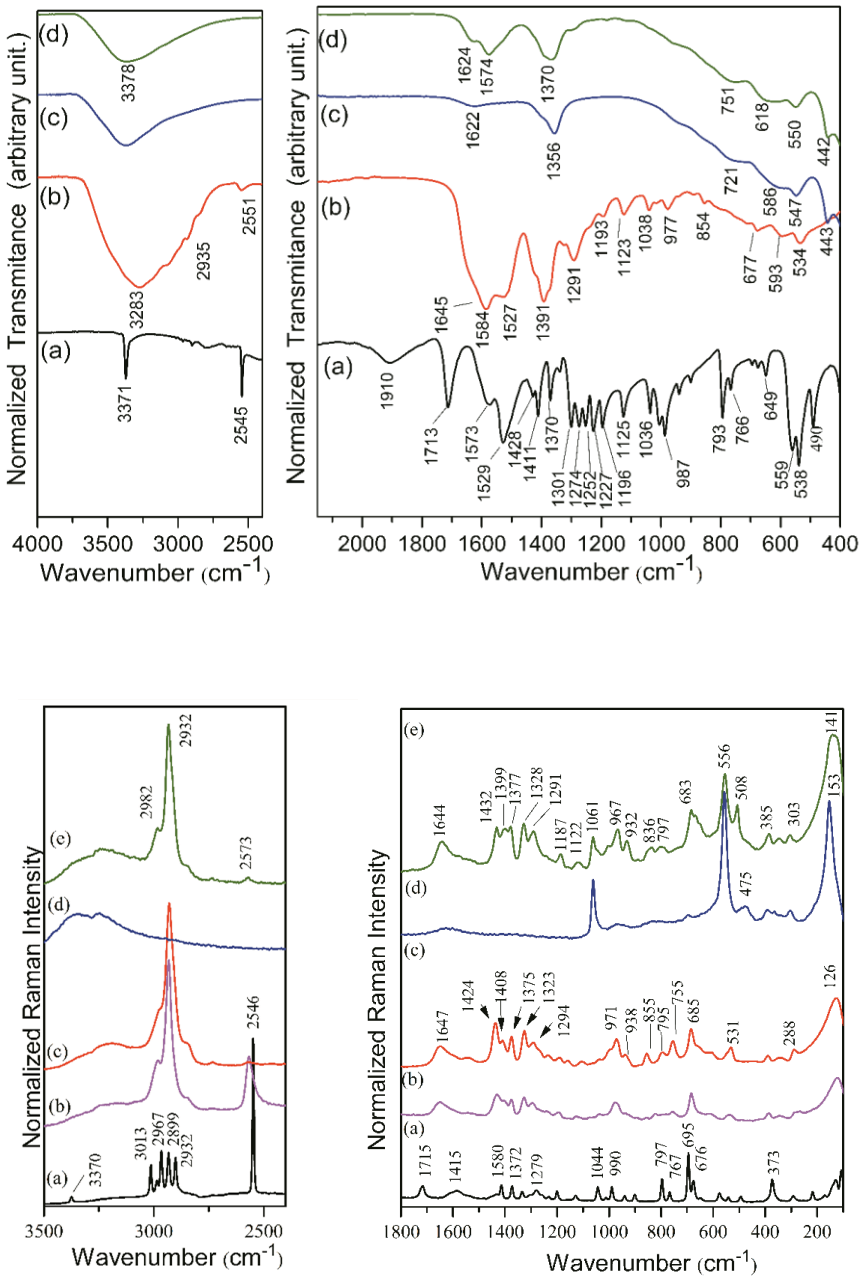

Figure S10. FTIR spectra (top) of (a) NAC, (b) NAC-pH=9.5, (c) Mg_2Al-Cl and (d) Mg_2Al-NAC, and FT-Raman spectra (down) of (a) NAC, (b) NAC-pH=9.5, (c) NAC-pH=11.0, (d) Mg_2Al-Cl and (e) Mg_2Al-NAC.

9. ^{13}C-CPMAS NMR spectra of NAC and Mg_2Al-NAC sample

As indicated in **Figure S11**, this work suggests that the resonance peak of the nuclei ^{13}C in the oxidized NAC (C*) is shifted as follows: C1* from 175.0 to 179.4 ppm, C3* from 28.3 to 36.9 ppm, C5* from 23.3 to 19.9 ppm. For the reduced NAC, C1 peak (177.2 ppm) is located at the same value as that for Zn_2Al-NAC55 material (177.8 ppm), but C2 and C3 peaks are distinct due to the *thiol* group oxidation. Additionally, the peak at 170.7 ppm (marked as C$^{\#}$ in Mg_2Al-NAC) is attributed to the LDH intercalated with carbonate ion [3] due to atmospheric CO_2 contamination.

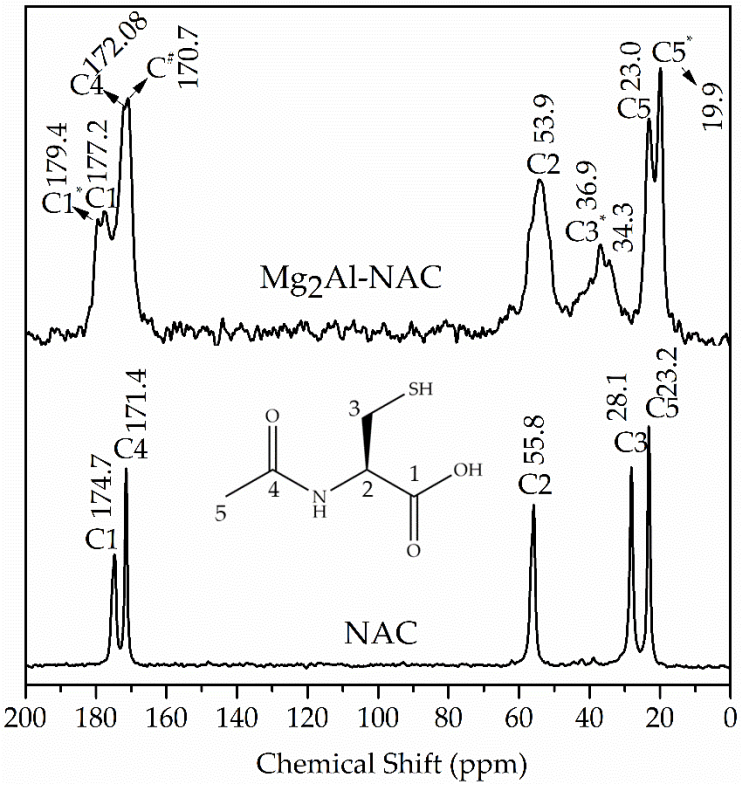

Figure S11. ^{13}C-CPMAS NMR spectra of NAC and Mg_2Al-NAC samples.

10. Kinetic models applied to the Zn_2Al-NAC55 sample

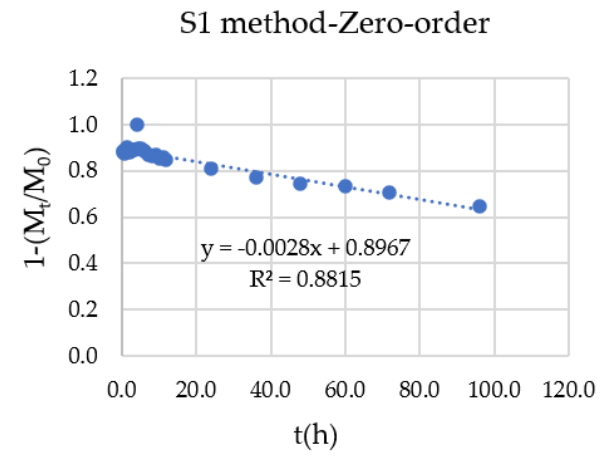

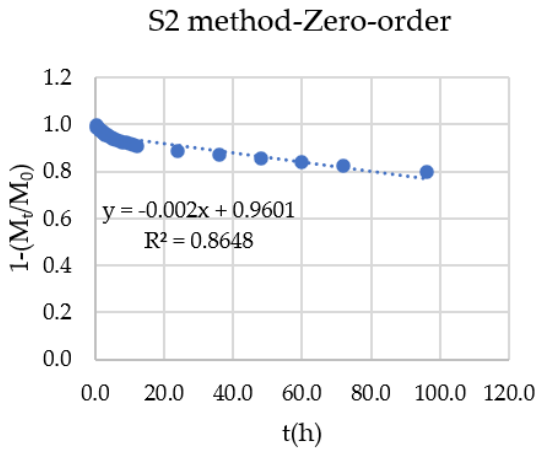

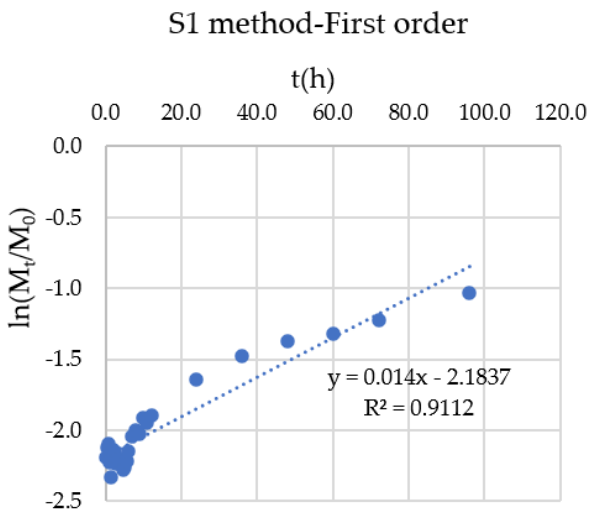

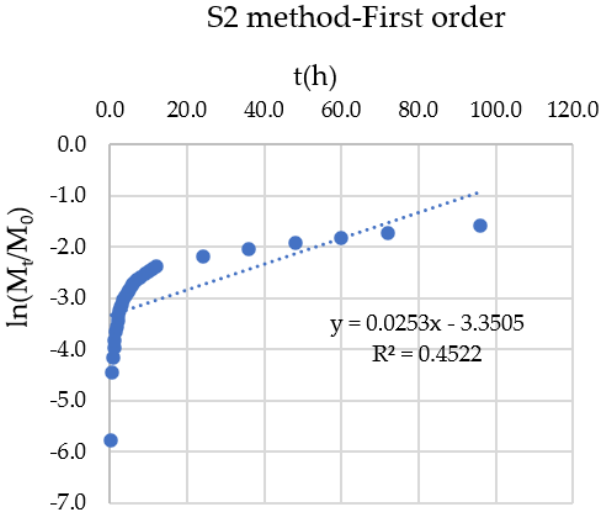

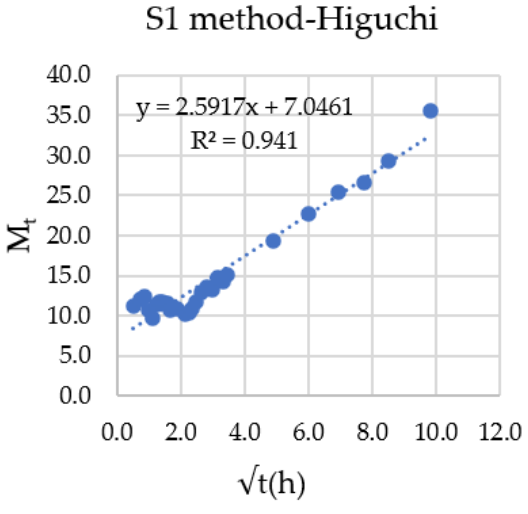

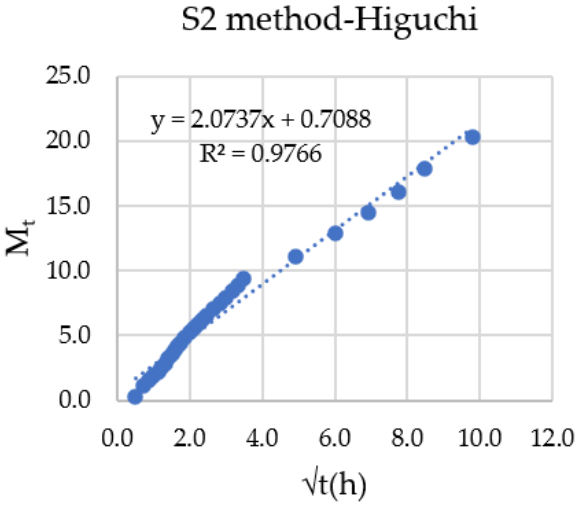

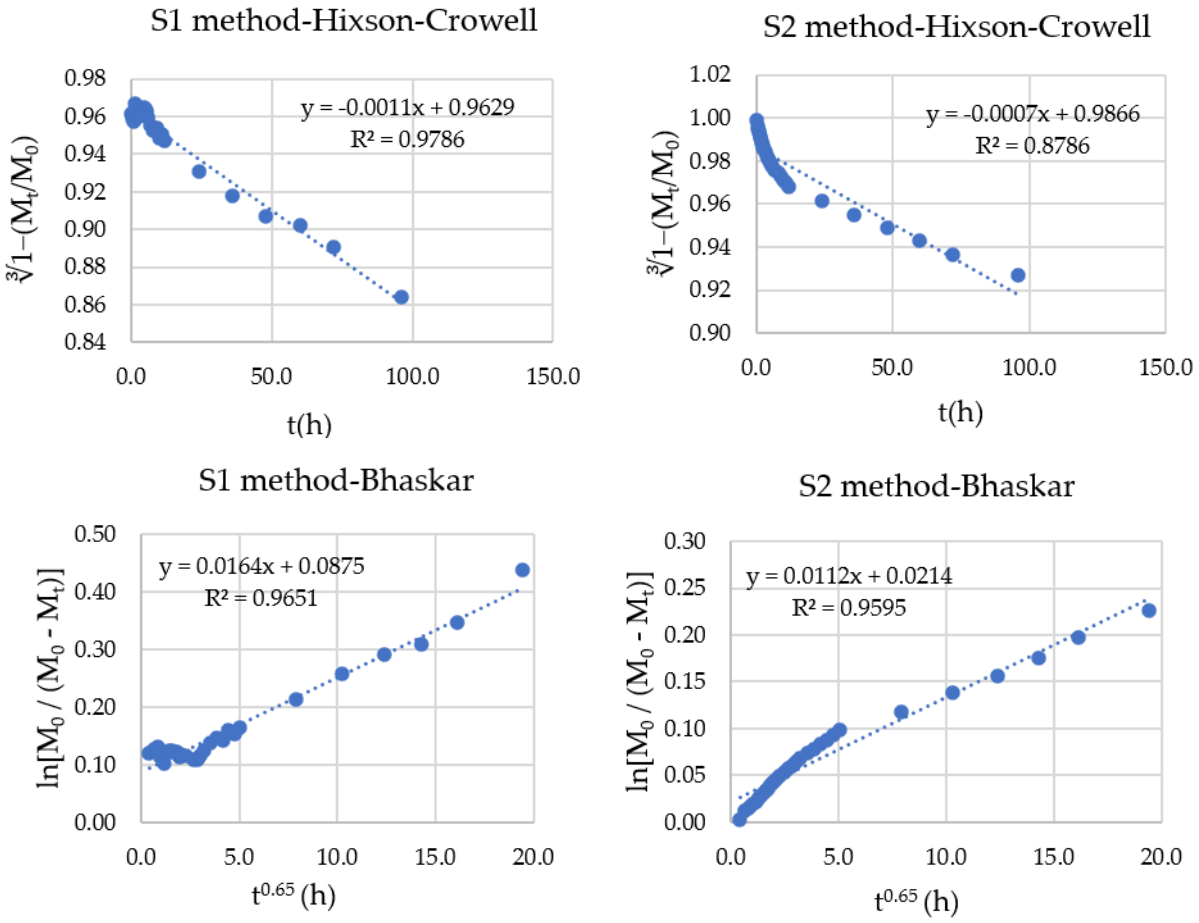

Figure S12. Kinetic models applied to the Zn_2Al-NAC55 sample, M_t is the amount of NAC released at time t and M_0 is the initial amount of NAC.

REFERENCES

1. Kumar, S.S.; Nangia, A. A New Conformational Polymorph of N-Acetyl-l-Cysteine. The Role of S–H···O and C–H···O Interactions. *CrystEngComm* **2013**, *15*, 6498, doi:10.1039/c3ce40879e.
2. Cunha, V.R.R.; de Souza, R.B.; da Fonseca Martins, A.M.C.R.P.; Koh, I.H.J.; Constantino, V.R.L. Accessing the Biocompatibility of Layered Double Hydroxide by Intramuscular Implantation: Histological and Microcirculation Evaluation. *Sci. Rep.* **2016**, *6*, 30547, doi:10.1038/srep30547.
3. Olszówka, J.E.; Karcz, R.; Kry, J.; Napruszewska, B.D.; Sulikowski, B.; Socha, R.P.; Gawe, A. New Insight into the Preferred Valency of Interlayer Anions in Hydrotalcite- like Compounds : The effect of Mg / Al Ratio. *Appl. Clay Sci.* **2018**, *155*, 84–94, doi:10.1016/j.clay.2018.01.013.